

Fracture process zone in high strength concrete

G.Appa Rao & B.K.Raghu Prasad

Department of Civil Engineering, Indian Institute of Science, Bangalore-560 012, India

ABSTRACT: An experimental investigation on the influence of maximum size of coarse aggregate, cement and coarse aggregate contents on the size of fracture process zone (FPZ) in high-strength concrete (HSC) is reported. Wide ranges of concrete mixes were designed to vary the compressive strength of concrete between 55 MPa and 80 MPa. Three different maximum sizes of coarse aggregates namely 10mm, 16mm, 20mm and combination of the above three were adopted. The size of FPZ was obtained qualitatively using ultrasonic pulse velocity technique. Single edge notched compact tension specimens (SENCTS) of size 500 mm x 500 mm x 80 mm with 250 mm edge notch subjected to uniform far field stress were used. It has been observed that the size of FPZ was influenced by the size of coarse aggregate. The size of FPZ increases as the maximum size of coarse aggregate increases up to 16 mm size and then tend to decreases with aggregate size. The size of FPZ was in the order of the magnitude of the size of coarse aggregate. It seems that the FPZ in HSC is localized indicating possible application of LEFM to HSC. Further, the FPZ decreases as the cement content increases, and relatively higher values of FPZ have been observed at higher coarse aggregate contents.

1. INTRODUCTION

Accurate experimental investigation of the fracture parameters of concrete is very important. Generally the fracture parameters are determined in the research laboratories on relatively small size specimens, which are significantly dependent on the specimen size. The structure of concrete is viewed as a multi-level hierarchy system (Zaitsev and Wittmann (1984)). The presence of inhomogeneities in concrete results in stress concentration at different interfaces of the system at higher stress levels. However, the information on the characteristics of fracture process zone (FPZ) and its extension in HSC are very limited. Research efforts have been reported to estimate the extent of FPZ using different techniques, which are classified under (i) Indirect or Non-destructive Techniques and (ii) Direct or Destructive Techniques. The non-destructive techniques are ultra sonic pulse velocity technique, acoustic emission technique, photo elastic coating techniques, laser speckle interferometry, Moire interferometry, holographic interferometry, compliance techniques, and infrared vibrothermography. These non-destructive techniques enable data collection during specimen loading. The destructive techniques

are based on the direct observation of material fracture using, optical microscopy, scanning electron microscopy, X- ray diffraction techniques, or high-speed photography. These techniques are limited to surface observations only.

2. FRACTURE PROCESS ZONE

Before the peak load, tip of a crack in concrete is characterized by cluster of microcracks, which is often known as fracture process zone (FPZ). Significant amount of fracture energy is absorbed in this zone due to large extent in conventional concrete. However, high strength concrete is more brittle and tend to behave more like a composite material due to strong interfacial bond between cement paste and aggregate, which lead to show localized FPZ in HSC. Hu and Wittmann (1992) introduced local fracture energy, which decreases in HSC due to very small FPZ. Two basic mechanisms take place in the softening regime of concrete (van Mier et al. (1990)). The post peak softening response of concrete and its ductility are primarily related to maximum size of coarse aggregate, grading of aggregates, and confinement stress on the test specimen (Rado-

vani (1990)). Mihashi et al. (1991) applied three-dimensional acoustic emission technique to study the FPZ. The results revealed that the micro cracking occurs randomly around the macro crack surface and the FPZ expands after the peak load due to the presence of aggregates. The beginning of descending branch in tension softening diagram corresponds to micro crack localization and extension and the tail the descending portion is attributed to the aggregate bridging. Mihashi and Nomura (1992) reported that the length of FPZ ahead of the notch tip is independent of the maximum size of coarse aggregate but the width of FPZ depends on the maximum size of coarse aggregate. Opara (1993) reported that the process zone in mortars was occurring as a cloud of unconnected micro-cracks around and ahead of a Mode I macro-crack, the length of which was about 150 mm and the width 20 mm. The maximum extent of FPZ was observed to be 100 mm, which is of the order of magnitude of the specimen dimension (Jankowski and Stys (1990)). The fracture processes in concrete involve (i) growth of de-bonding cracks near large aggregates, (ii) growth of a continuous macro-crack and (iii) failure of interface along the grain boundaries (van Mier (1991)). The coarse aggregate particles arrest crack propagation and cause crack branching. The crack length at ultimate loads was observed to be about 15-20 mm (Horii and Ichinomiya (1991)). Damage measurements in concrete through ultrasonic pulse velocity technique were found to be useful to evaluate defects, micro-structure and residual stresses (Keating et al. (1989), Tharmaratnam and Tan (1990), Berthaud (1991), Bungey (1989), Selleck et al. (1998), Raj et al. (1996)).

Otsuka and Date (2000) observed that the fracture crack zone size increases as the size of test specimen increases. Further, the dimension of FCZ, at the peak load and the 70 % of the peak in the post-peak regime, developed after the peak load with larger uncracked ligament length, with short ligament length, the FCZ did not develop so sufficiently. Zhang and Wu (1999) studied the FPZ in HSC using beam specimens, in which the notch depth was varied from 20 to 80mm. As the notch depth increases, the fracture process in concrete beam becomes less catastrophic and for smaller crack lengths, the FPZ increases linearly with the crack extension. As the crack extends to half of the ligament, the FPZ size reaches its maximum size and saturated. Thereafter, the FPZ moves ahead and shrinks to about 0.77 times that of the uncracked ligament depth. Wittmann and Hu (1991) reported that at the maximum load, the FPZ length is around 23mm and the width

was 12mm. Alexander and Blight (1990) observed that the FPZ in smaller beams is very small, which reaches a steady state length. The size of fracture process zone varies between 38 and 37 mm for three-point bend specimens and between 38 and 64 mm for compact tension specimens. Beyond the steady state, the FPZ size diminishes due to both the edge effects and compressive stress fields that restrain its free growth (Gopalathnam and YE (1991)). The formation of FPZ occurs between 80 % of pre-peak load and 80 % of post-peak load (Li and Shah (1994)). The FPZ inclined with the initial crack due to the presence of aggregate and in small specimens the ligament length was insufficient to permit the FPZ to fully develop (Du et al. (1987)).

3. DETERMINATION OF FPZ

The following expression has been used to estimate the size of fracture process zone in the present program.

$$a = a_0 + \Delta a = a_0 + \left[\frac{V_{p,f}}{V_{p,i}} - 1 \right] (l_i) \dots \dots \dots (3.1(a))$$

$$FPZ = a - a_0 = \left[\frac{V_{p,f}}{V_{p,i}} - 1 \right] (l_i) \dots \dots \dots (3.1(b))$$

Where FPZ = fracture process zone (mm), $V_{p,f}$ = mean ultrasonic pulse velocity, km/sec at any load P_f , $V_{p,i}$ = mean ultrasonic pulse velocity, km/sec before the application of the load, l_i = length of the diagonal from a reference grid point to the initial notch tip (mm). The pulse velocity was calculated using the thickness of the specimen divided by the time of ultrasonic pulse traveled. The measurements were made using direct method, in which the pulses traveled normal to the plane of the specimen. The direct method is relatively better for estimating the extent of damage in the concrete. At every load increment, the mean ultrasonic pulse velocity among all the grid points was determined and the FPZ was estimated using eqs. (3.1).

4. EXPERIMENTAL PROGRAM

4.1 Materials

Ordinary Portland cement was used for the program. Sand was natural river sand passing through 2.36 mm sieve, whose specific gravity was 2.67. Coarse

aggregate was crushed white granite with specific gravity 2.65. Potable water was used with superplasticizer for mixing the concrete. The water-cement ratio was 0.30 throughout the program. Constituent materials in different concrete mixes in Series-I and II respectively are shown in Tables 1 and 2.

Table 1: Constituent materials in different concretes in Series-I.

Mix Designation	Coarse Aggregate Size (mm)	Cement Content (kg/m ³)	Sand Content (kg/m ³)	CA Content (kg/m ³)
410-A	10	400	800	1200
416-A	16	400	800	1200
420-A	20	400	800	1200
460-B	10	450	800	1200
466-B	16	450	800	1200
470-B	20	450	800	1200
510-C	10	500	800	1200
516-C	16	500	800	1200
520-C	20	500	800	1200
415-D	M	400	800	1200
465-D	M	450	800	1200
515-D	M	500	800	1200

Table 2: Constituent materials in different concretes in Series-II.

Mix designation	Coarse Aggregate Size (mm)	Cement Content (kg/m ³)	Sand Content (kg/m ³)	CA Content (kg/m ³)
860-E	10	450	700	850
960-E	10	450	700	950
1060-E	10	450	700	1050
866-F	16	450	700	850
966-F	16	450	700	950
1066-F	16	450	700	1050
870-G	10	450	700	850
970-G	16	450	700	950
1070-G	20	450	700	1050

4.2 Testing of Specimens

In order to measure the size of fracture process zone ultra sonic pulse velocities at different grid points on the specimen surface were measured. The grids were formed at 75 mm x 100 mm spacing in the test specimen. A total of nineteen grid points, including one grid point at the notch tip, were formed at different locations symmetrically with reference to the single edge notch. At every load increment, the time traveled through the thickness of the test specimen at every grid point was recorded and the pulse velocity was calculated dividing the distance traveled by the time. The ultrasonic pulse velocity was measured using portable ultrasonic non-destructive digital indicating tester (PUNDIT).

5. TEST RESULTS AND DISCUSSION

5.1. Variation of Fracture Process Zone with maximum size of coarse aggregate

Fig. 1 shows a typical variation of fracture process zone (FPZ) with applied load in HSC. The variation of load with FPZ shows that the fracture process

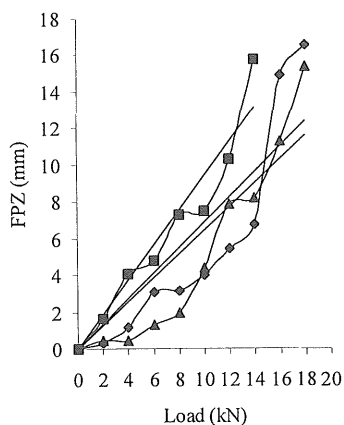


Fig. 1: Typical diagram showing the variation of FPZ with load in HSC.

zone length increases as the load on the test specimen increases. Fig. 2 shows the variation of FPZ with maximum size of coarse aggregate. At every cement content i.e. at 400, 450 and 500 kg/m³, three maximum sizes of coarse aggregates 10, 16 and 20 mm were used. It has been observed that the FPZ increases up to the aggregate size of 16 mm, thereafter, the FPZ shown to decrease with maximum size of coarse aggregate in concrete mixes with 400 and 500 kg/m³ cement contents. Whereas, at 450 kg/m³, the size of FPZ has been observed to increase with the maximum size of coarse aggregate up to 20 mm size. Three-dimensional acoustic emission technique has been adopted to study the fracture process zone of concrete on double cantilever beam specimens (Mihashi et al. (1991a)). The fracture process zone expanded after peak loads due to the presence of aggregates. Mihashi et al. (1991b) observed that the beginning of descending branch corresponds to micro crack localization and extension Mihashi and Nomura (1992) observed that the length of FPZ ahead of the notch tip is independent of the maximum size of coarse aggregate but the width of FPZ depends on the maximum size of coarse aggregate. The maximum extent of fracture process zone was observed to be 100 mm, which is of the order of magnitude of the specimen dimension (Jankowski

and Stys (1990)). The micro-cracking zone rapidly increases at the range of 0.70-1.0 of ultimate load. The coarse aggregate particles arrest crack propagation and cause crack branching. The crack length at ultimate loads was observed to be about 15-20 mm (Horii and Ichinomiya (1991)). Otsuka and Date (2000) observed that the width of the fracture crack zone increases with the increase of aggregate size. In the case of short ligament lengths, the FCZ did not develop so sufficiently. It was suggested that the short ligament seems to be not appropriate to develop the FCZ completely.

5.2. *Variation of Fracture Process Zone with cement content*

Fig. 3 shows the variation of FPZ with cement content using different coarse aggregate sizes. It demonstrates that the concrete with 10 mm coarse aggregate at 450 kg/m³ of cement content exhibit the lowest value of FPZ. It clearly shows that the concrete with 10 mm size coarse aggregate at 450 kg/m³ of cement content exhibit very good homogeneity and composite behavior. This is due to strong interfacial bond strength between cement paste and coarse aggregate, which results in the smallest size

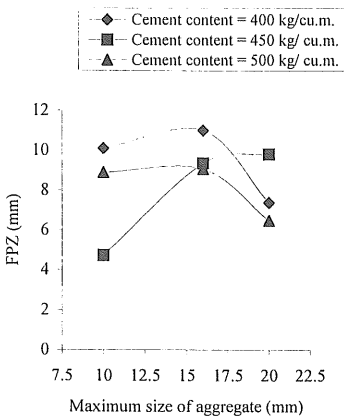


Fig. 2: Variation of FPZ with maximum size of coarse aggregate.

of process zone in front of the crack tip. In the concrete mixes with 16 mm size coarse aggregate, the size of FPZ ranges between 9 and 11 mm. However, using 20 mm coarse aggregate, the size of FPZ was ranged between 7 and 10 mm. From the above observations, it has been noticed that the stronger concrete mixes containing relatively smaller size inhomogeneity exhibited slightly lower values of the FPZ. The cement content i.e. 450 kg/m³ seems to be

the optimum content at which lowest values of FPZ were noticed.

5.3. *Variation of Fracture Process Zone with coarse aggregate content*

The influence of coarse aggregate content combined with the maximum size of coarse aggregate is shown in Fig. 4. It clearly demonstrates that the size of FPZ in HSC was slightly influenced by the coarse aggregate content. In general, it has been observed that the lowest values of FPZ were noticed with 10 mm coarse aggregates and the highest with 20 mm size. However, at a coarse aggregate content of 850 kg/m³, concrete with 16 mm size exhibited the highest value of 20 mm among all other concrete mixes. Using 10 and 16 mm coarse aggregates, the FPZ slightly decreases with the coarse aggregate content up to 950 kg/m³, there after, it has been shown to increase slightly with the coarse aggregate content. Moreover, the size of FPZ in HSC with 20 mm coarse aggregate size is about 16.5 mm. It has been generally noticed that the concrete mixes containing large size coarse aggregate at higher coarse aggregate contents exhibited larger size process zone in front of the crack tip in HSC.

From the above observations, it has been clearly noticed that the size of FPZ is influenced by various parameters and the mix proportions. Stronger concrete mixes exhibited linear variation of FPZ with load up to 90 percent of the ultimate load and the size of FPZ seems to be very small, which localized around the crack tip. However, it may be difficult to make precise conclusions regarding the size of FPZ, because the FPZ was calculated using a crude way of analysis. The FPZ have been calculated using the

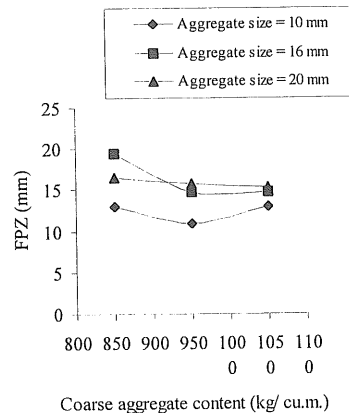


Fig. 4: Variation of FPZ with coarse aggregate content.

mean values of ultrasonic pulse velocity at different points at the grid points formed in the test specimen, under far field stress conditions. Though the size of FPZ increases as the load increases, the maximum size of the FPZ is of the order of the magnitude of the size of the maximum size of coarse aggregate. The size of FPZ has been observed to be larger at lower cement contents using smaller size coarse aggregate, while it is higher at higher cement contents using larger size coarse aggregate. This may be explained by using the specific surface of aggregate to cement ratio. At higher cement contents, the interface between the coarse aggregate and the cement paste is thin with smaller size aggregate, due to larger surface area. Therefore, a good transfer of stress from the aggregate to the paste could be possible. Whereas, in the case of concrete with larger size aggregate, the thickness of the interface increases, which results in crushing of cement near the aggregate contact points. This may lead to damage of concrete surrounding the crushing points, which results in the extension of damage in to the concrete.

6. LIMITATIONS

The values obtained using this technique have few limitations.

- (i). The material throughout the test specimen is perfectly elastic up to the ultimate load.
- (ii). The stress at the notch tip up to the load just before the ultimate is assumed as progressively increasing as the load is increasing.
- (iii). At the load level of 90 percent of the ultimate, the stress near the crack tip reaches its limiting strength.
- (iv). The stress in the major portion of the test specimen except at the crack tip has been released, due to the concentration of whole energy near the crack tip.

7. CONCLUSIONS

The FPZ seems to be influenced by the maximum size of coarse aggregate. The FPZ in HSC is in the order of magnitude of the size of coarse aggregate. The FPZ increases with coarse aggregate size up to about 16 mm size, thereafter it decreases. At higher cement contents, due to strong interface in HSC, the size of FPZ seems to be small. However, at higher coarse aggregate contents, the size of FPZ seems to

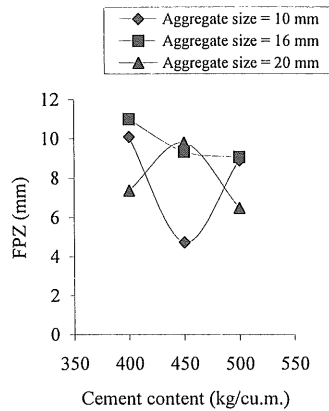


Fig. 3: Variation of FPZ with cement content.

be on the higher side. Due to very localized extent of FPZ in HSC, therefore, it may be very nearer for direct applicability of LEFM to HSC.

8. REFERENCES

- Alexander, M.G., and Blight, G.E. 1990. Behavior of fracture process zones in notched concrete beams, *International Journal of Fracture*, 44: 71- 77.
- Berthaud, Y. 1991. Damage Measurements in Concrete Via an Ultrasonic Technique. Part I Experiment, *Cement and Concrete Research*, 21(1): 73-82.
- Bungey, J.H. 1989. Testing of Concrete in Structures, Surrey University Press, USA, Chapman and Hall, New York, 2nd Edition, 40-64.
- Du, J.J., Kobayashi, A.S., and Hawkins, N.M., 1987. Fracture process zone of a concrete fracture specimen, Ed. S.P. Shah and S.E. Swartz) *RILEM Intl. Conference on Fracture of Concrete and Rock*, Houston, Texas, June 1987, 199-201.
- Gopalarathnam, V.S., and YE, B.S., 1991. Numerical characterization of the nonlinear fracture process in concrete, *Engineering Fracture Mechanics*, 40(6): 991-1006.
- Horii, H., and Ichinomiya, T. 1991. Observation of Fracture Process Zone by Laser Speckle Technique and Governing Mechanism in Fracture of Concrete, *Current Trends in Concrete Fracture Research*, Kluwer Academic Publishers, pp.19-29.
- Hu, X.Z., and Wittmann, F.H. 1992. An Analytical Method to Determine the Bridging Stress Transferred within the Fracture Process Zone:II, Application to Mortar, *Cement and Concrete Research*, 22: 559-570.
- Hu, X.Z., and Wittmann, F.H. 1992. Fracture Energy and Fracture Process Zone, *Materials and Structures*, 25: 319-326.
- Jankowski, L.J., and Stys, D.J. 1990. Formation of the Fracture Process Zone in Concrete, *Engineering Fracture Mechanics*, 36(2): 245-253.
- Keating, J., Hannant, J., and Hibbert, A.P. 1989. Correlation Between Cube Strength, Ultrasonic Pulse Velocity and Volume Change for Oil Well Cement Slurries, *Cement and Concrete Research*, 19: 715-726.
- Li, Z., and Shah, S.P. 1994. Localization of Microcracking in

- Concrete Under Uniaxial Tension, *ACI Materials Journal*, 91(4): 372-381.
- Mihashi, H., Nomura, N.; and Niiseki, S. 1991a. Influence of Aggregate Size on Fracture Process Zone of Concrete Detected with Three Dimensional Accoustic Emission Technique, *Cement and Concrete Research*, 21: 737-744.
- Mihashi, H., and Nomura, N. 1992. Micro-cracking and Tension-Softening Properties of Concrete. , *Cement and Concrete Composites*, 14: 91-103.
- Nomura, N., Mihashi, H., and Izumi, M. 1991b. Correlation of Fracture Process Zone and Tension Softening Behavior in Concrete, *Cement and Concrete Research*, 21: 545-550.
- Opara, N.K. 1993. Fracture Process Zone Presence and Behavior in Mortar Specimens, *ACI Materials Journal*, 90(6): 618-626.
- Otsuka, K., and Date, H. 2000. Fracture process zone in concrete tension specimen, *Engineering Fracture Mechanics*, 65: 111-131.
- Radovani, B.A. 1990. Grain Size of Adopted Aggregate Influence on Strain-Softening of Concrete, *Engineering Fracture Mechanics*, 35 (415): 709-718.
- Raj, B., Jayakumar, T., and Palanichamy, p. 1996. Ultrasonic Non Destructive Evaluation for Defects, Micro Structures and Residual Stresses, *Proceedings of Seventh National Symposium on Ultrasonics, India*, 21-29.
- Selleck, S.F., Landis, E.N., Peterson, M.L., Shah, S.P., and Achenbach, J.D. 1998. Ultrasonic Investigation of Concrete with Distributed Damage, *ACI Materials Journal*, 95(1): 27-36.
- Tharmaratnam, K., and Tan, B.S. 1990. Attenuation of Ultrasonic Pulse in Cement Mortar, *Cement and Concrete Research*, 20: 335-345.
- Van Mier, J.G.M. 1991. Mode I Fracture of Concrete: Discontinuous Crack Growth and Crack Interface Grain Bridging, *Cement and Concrete Research*, 21: 01-15.
- van Mier, J.G.M., and Nooru-Mohamed, M.B. 1990. Geometrical and Structural Aspects of Concrete Fracture , *Engineering Fracture Mechanics*, 35(4/5): 617-628.
- Wittmann, F.H., and Hu, X.Z. 1991. Fracture Process Zone in Cementitious Materials, *Current Trends in Concrete Fracture Research*, (Edited by) Z.P.Bazant, Kluwer Academic Publishers, Printed in the Netherlands, pp.03-18.
- Zhang, D., and Wu, K. 1999. Fracture process zone of notched three-point bending concrete beams, *Cement and Concrete Research*, 29: 1887-1892.
- Zaitsev, Y.B., and Wittmann, F.H. 1984. Simulation of Crack Propagation and Failure of Concrete, *Materials and Structures*, 14(83): 357-365.